APPLICATION OF THE FABRY-PEROT INTERFEROMETER TO ABSORPTION SPECTROSCOPY

A THESIS

Presented to

the Faculty of the Division of Graduate Studies

Georgia Institute of Technology

In Partial Fulfillment

of the Requirements for the Degree

Master of Science in Chemistry

by

Walter William Moseley, Jr.

June 1951

240699
Crosskand

AR 7-10-51

APPLICATION OF THE FABRY-PEROT INTERFEROMETER TO ABSORPTION SPECTROSCOPY

Approved:

Date Approved by Chairman Jun. 5, 1951

ACKNOWLEDGMENTS

I wish to express my sincerest gratitude to Dr. W. H. Eberhardt, both for suggesting this problem, and for his valuable aid and assistance throughout its prosecution. I should also like to extend my appreciation to Dr. Vernon Crawford and the School of Physics for permitting the use of the Bausch and Lomb Large Littrow Spectrograph.

TABLE OF CONTENTS

LIST OF TABLES

LIST OF FIGURES

APPLICATION OF THE FABRY-PEROT INTERFEROMETER TO ABSORPTION SPECTROSCOPY

I

SUMMARY

An attempt has been made to determine the practicability of crossing the dispersion of a Fabry-Perot interferometer with that of the Bausch and Lomb Large Littrow Spectrograph to obtain greater resolution and dispersion for the study of molecular absorption than is ordinarily possible. Even though some studies of this technique have been made for monochromatic absorption, no research has been reported for more complex systems and little attempt has been made to correlate the details of the spectrogram produced in this manner with the characteristics of the interferometer, spectrograph, and photographic plate.

From fundamental equations expressing the behavior of the interferometer and spectrograph separately, equations were derived to determine the effect on the spectrogram of the following factors: slit width of the spectrograph, spectrographic dispersion, reflection coefficient of the interferometer plates, resolv-

ing power of the photographic plates, and temperature and pressure changes during an exposure. From the theoretical study, it was possible to specify the precise requirements that an interferometer places on a spectrograph and to develop both an understanding of what features should appear in the absorption spectrum and to derive more accurate equations for converting measurable quantities into wave numbers of absorption bands.

The channelled spectrogram produced with a continuous source of radiation and very small slit width is known to consist of a series of closely spaced almost vertical parabola segments with the distance, ΔS, along the dispersion of the spectrograph between these given by the equation

$$\Delta S = \frac{\lambda^2}{2td}$$

where t in this equation is the distance between the interferometer plates, d is the dispersion of the spectrograph, and λ is the wave length of the region under consideration. For infinitely sharp interference fringes, the channels just disappear to give a continuous background when the slit width is equal to ΔS, and overlap with a reduction in resolution when the slit width is larger than this value. For finite fringes the critical slit width required to produce the continuous background

is dependent upon the fringe width. Since it is desired to use the largest slit width consistent with maximum resolution, this condition represents the optimum operating conditions for studies of absorption spectra. The above equation then forms the basis for the specification of requirements on the spectrograph and interferometer.

The limit of resolution of the interferometer-spectrograph combination operated in this condition is determined entirely by that of the interferometer which is simply related to the interferometer spacing and the reflection coefficient of the plates. For an interferometer spacing of 0.15 cm as used in this work and a reflection coefficient assumed to be at least 0.80, the theoretical resolving limit of the interferometer was calculated as 0.04 Å. In the region of 4,000 Å, this corresponds to a resolving power of 1×10^5. From equations derived for the vertical distance between parabola segments for the optical system used in this study, the dispersion of the channelled spectrum normal to the spectrographic dispersion was calculated to be about 0.5 Å /mm. Since the resolving power of most photographic plates is approximately 50 lines/mm or 0.02 mm/line, the calculated resolution should be obtainable with ordinary plates, a relatively large slit width, and acceptable exposure times.

General equations derived to determine the extent

of the parabola broadening due to temperature and pressure changes during an exposure led to the conclusion that for the apparatus used in this study a control of temperature and pressure within 2° C and 4mm Hg would be sufficient for very accurate work. However, ordinary changes in room temperature and atmospheric pressure should be of little consequence for most work.

The results of these considerations have been confirmed by an experimental study of the absorption spectrum of nitrogen dioxide in the region around 4,000 Å. The maximum resolving limit attained was 0.24 Å which corresponds to a resolving power of 0.2×10^5. This limitation was ascribed to the actual width or complexity of the absorption bands which prevented further resolution.

An important limitation in the use of the channelled spectrum for absorption work is the tediousness inherent in the interpretation of the spectrogram which is now essentially a two-dimensional rather than the usual linear record. The increase in resolution was, however, clearly evident and served to accentuate many of the features of the spectrum which otherwise escaped observation. In addition, the wave number differences of absorption features were determined with considerable accuracy from the expression

$$\Delta\tilde{\nu} = \frac{\Delta m}{2t}$$

where Δm is the number of orders (parabola segments) between the absorption features.

It appears therefore, that the use of the interferometer-spectrograph combination is practicable and permits a more detailed and accurate determination of fine structure but for any but the simplest spectra presents a problem of interpretation of very great difficulty.

II

INTRODUCTION

In the investigation of excited electronic states of polyatomic molecules, it is necessary to obtain greater resolution and dispersion than that which can be furnished by instruments now available at the Georgia Institute of Technology. For such studies in the region of 4,000 Å, it is desired to measure energy differences of about 0.1 cm^{-1}, or wave length differences of about 0.02 Å. Such measurements require a resolving power of the order of 2×10^5. Even though the Bausch and Lomb Large Littrow Spectrograph with glass optics has a theoretical resolving power of 1×10^5 in this region, it has a linear dispersion of only 5 Å/mm. Consequently, a slit width of about 8 μ would be required to realize this resolution. Such a small slit width would require relatively enormous exposure times and also place extreme demands on the resolving power of the photographic plate which is normally less than 50 lines/mm.

It seemed possible, however, that the required resolving power and dispersion could be obtained by crossing a Fabry-Perot interferometer with the Bausch

and Lomb Large Littrow Spectrograph available in the School of Physics. This investigation has been undertaken to determine the practicality of such a technique.

Although the application of the Fabry-Perot interferometer to monochromatic absorption has been studied in considerable detail[1, 2, 3] there seemed to be no publications in which the Fabry-Perot instrument was used for the study of molecular absorption. Furthermore, little attempt was found in the literature to correlate the details of the spectrogram produced by a continuous source with the characteristics of the crossed instruments to the degree that seemed necessary for the type of measurement undertaken in this study.

---

[1] Karl Wilh.Meissner, Journal of the Optical Society of America 32 p. 191 (1942)

[2] Chas. Fabry, Comptes Rendus 140, 1136 (1905); Chas. Fabry, H. Buisson, Journal de Physics et le Radium 9, 197 (1910)

[3] K. Burns and Wm. F. Meggers, Publications of the Allegheny Observatory of the University of Pittsburgh, 6, 105, (1925)

III

DESCRIPTION OF THE FABRY-PEROT INTERFEROMETER

The Fabry-Perot interferometer consists of two partially metallized plates, A and B, placed one behind the other, so that rays of light, I, passing through the plates in sequence will be partially reflected at both as shown in Figure 1.

The distance between the plates, usually of the order of a few millimeters, is rigidly fixed since it must be accurately known for most experiments. The plates are usually quartz or glass discs coated with a metal that exhibits, in the desired wave length region, a high reflection coefficient in the solid state and a high transparency as a thin film. Thus, by properly coating the plates, the desired degree of reflection may be obtained. Tolansky[4] discusses the characteristics of various kinds of plates in considerable detail.

The interferometer used in this study is a commercially available instrument manufactured by the Gaert-

---

[4] S. Tolansky, High Resolution Spectroscopy (New York: Pitman Publishing Corporation, 1947) p. 104

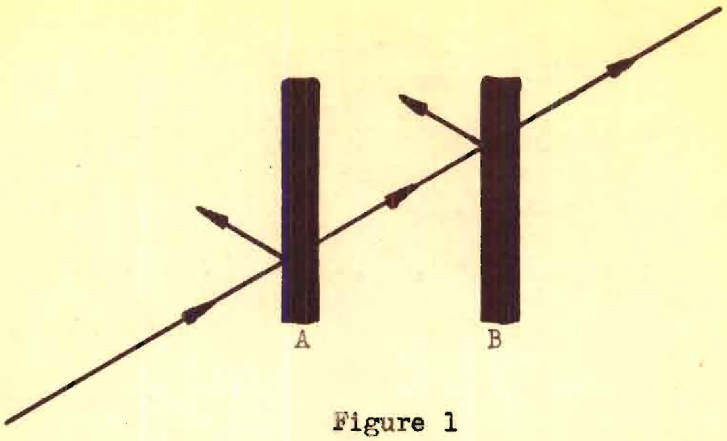

Figure 1

INTERFEROMETER PLATES

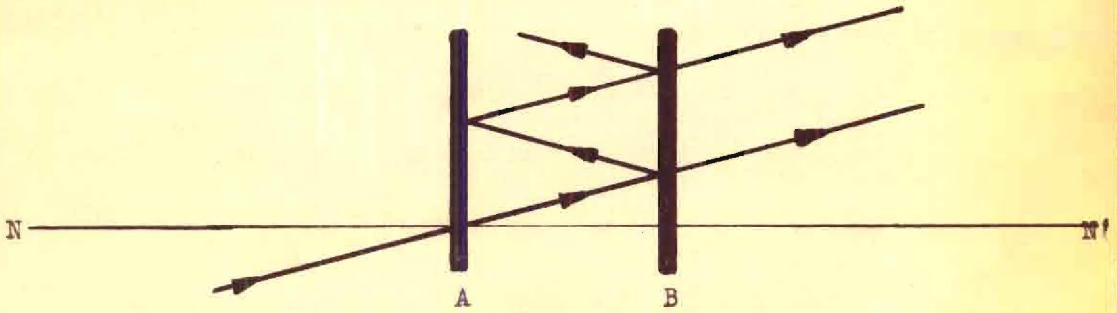

Figure 2

TRANSMISSION AND REFLECTION IN THE

FABRY-PEROT INTERFEROMETER

ner Scientific Company, under the catalogue number L2320Q. The plates, which are of quartz, are 27 mm in diameter and about 5 mm in thickness with surfaces ground flat to better than 1/20 th wave length. The front and back surfaces of each plate are inclined at a small angle to each other to prevent spurious interference.[5, 6]

The plates are mounted in a brass holder with a fixed spacer. As originally designed, the spacer is a quartz annular ring 10.030 mm in thickness. This spacing gives good resolving power for discrete spectra, but produces a pattern for continuous spectra which is not adaptable to the Bausch and Lomb instrument. (See section on requirements of the spectrograph). In order to obtain a suitable pattern, the quartz spacer was replaced by three 1/16 inch ball bearings held loosely in a ring of 1/32 inch lucite. The bearings were sufficiently uniform in diameter to allow sharp, uniform patterns to be obtained with monochromatic radiation.

---

[5] Ibid., p. 145

[6] Harrison, Lord, and Loofbourow, Practical Spectroscopy (New York: Prentice Hall, Inc., 1948) p. 561

IV

THEORY OF THE FABRY-PEROT INTERFEROMETER

Figure 2 illustrates that the part of an incident ray, I, that is reflected at plate B of the interferometer will undergo repeated reflections between the plates, being partially transmitted upon each reflection at plate B to produce the series of parallel rays, T_{θ_1}. The nature of all such transmitted rays may be discussed in the following manner:

If a monochromatic ray I of wave length λ strikes the second plate of a Fabry-Perot interferometer (Figure 2) making an angle θ_1 with NN', the normal to the plates, a series of in-phase parallel rays will be transmitted also at an angle θ_1 with respect to the normal if θ_1 satisfies the equation:

$$2t \cos \theta = n\lambda \quad (I)$$

where n is any integer less than $2t/\lambda$, and t is the distance between the plates. Any incident ray parallel to I will produce transmitted rays identical in phase and direction with those produced by I.

All rays incident to plate B at an angle θ_1 define the surface of a family of cones F_{θ_1} of semi-angle

θ_1 perpendicular to B with apices in the plane of B. Any given ray on the surface of one such cone is parallel to one and only one ray in each of the remaining cones in the family. All the rays transmitted from one such group of parallel incident rays will be in phase and parallel and will therefore meet in a point at infinity. Any other group of parallel incident rays lying on the surfaces of the cones F_{θ_1} will be transmitted to produce rays meeting in a different point at infinity. The totality of all such points will describe a circle C_{θ_1} at infinity while the rays lying on the surfaces of another family of cones F_{θ_2} will produce a circle C_{θ_2} concentric with C_{θ_1} if θ_2 satisfies equation I.

It is possible to get an expression containing the diameter of these concentric circles when they are focused onto a screen. It has been shown that

$$m = m_o + e = \frac{2t}{\lambda} + \frac{2tD^2}{8 \lambda f2} \quad \text{(II)}$$

where m, a large integer, is the order of interference for the ring of diameter D, m_o is the integral order of interference for a ring of diameter D_o, which is equal to zero, e is the partial order of interference between the center and the first ring, f is the focal length of the lens used to focus the rings, and t is the distance between the interferometer plates.

From equation II it is seen that for two slightly different values of λ, two circles of slightly different diameters will be formed for each value of m. However, for a given value of λ two successive integral values of m correspond to two circles with appreciably different diameters. The interference pattern of two slightly different wave lengths for four values of m is shown in Figure 3 where two different series of concentric circles correspond to two different values of λ.

Finally, for a spectrum of discrete lines, the pattern consists of several series of concentric circles superimposed upon each other, each series corresponding to a single spectral line; each circle in a given series corresponding to a definite order m.

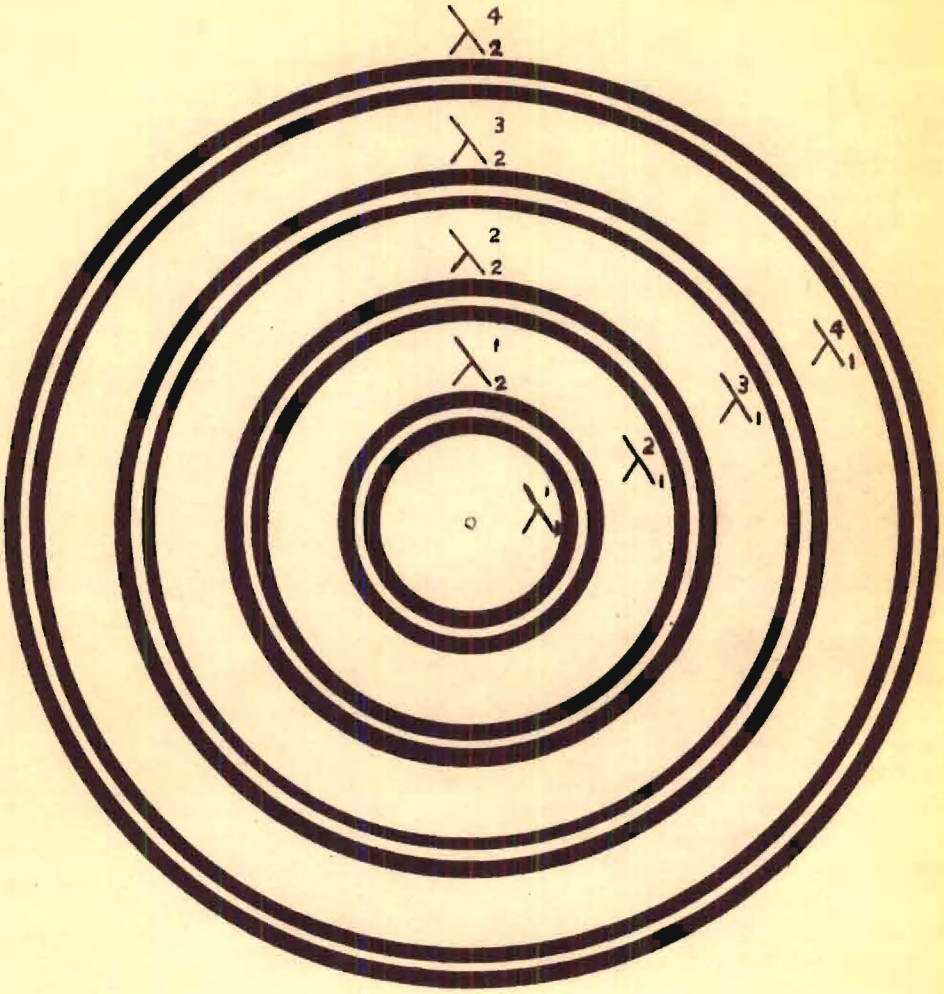

Figure 3

INTERFEROMETER PATTERN FOR TWO WAVE LENGTHS

IN FOUR ORDERS

Superscripts on λ indicate orders while subscripts indicate wave length values.

V

THEORY OF THE INTERFEROMETER SPECTROGRAPH PATTERN

The interferometer may be used in conjunction with a spectrograph as shown in Figure 4. Light entering the interferometer may or may not be parallel but the interference rings must be focused sharply on the spectrographic slit by a high quality achromatic lens L_2. By so focusing the fringes on the slit, only an arc of each circle is allowed to pass through the spectrograph as diagrammed in Figure 5a. The spectrograph produces the pattern diagramed in Figure 5b for a monochromatic source, but if the source consists of a mixture of two sufficiently different wave lengths, λ_1 and λ_2, the spectrograph produces the pattern diagramed in Figure 5c. As the slit is made smaller, the fringe arc becomes correspondingly smaller and approaches a point, Figure 5d. The effect shown in Figure 5c is illustrated in Figure 6 for the yellow mercury lines; the two sets of fringes which are not resolved by the spectrograph result from the presence of two mercury isotopes in the source.

The quantity D in Figure 5d, the diameter of a

Figure 4

INTERFEROMETER-SPECTROGRAPH OPTICAL SYSTEM

A	Source	FP	Interferometer
L_1	Converging	L_2	Ring Focusing Lens
S	Spectrograph Slit		

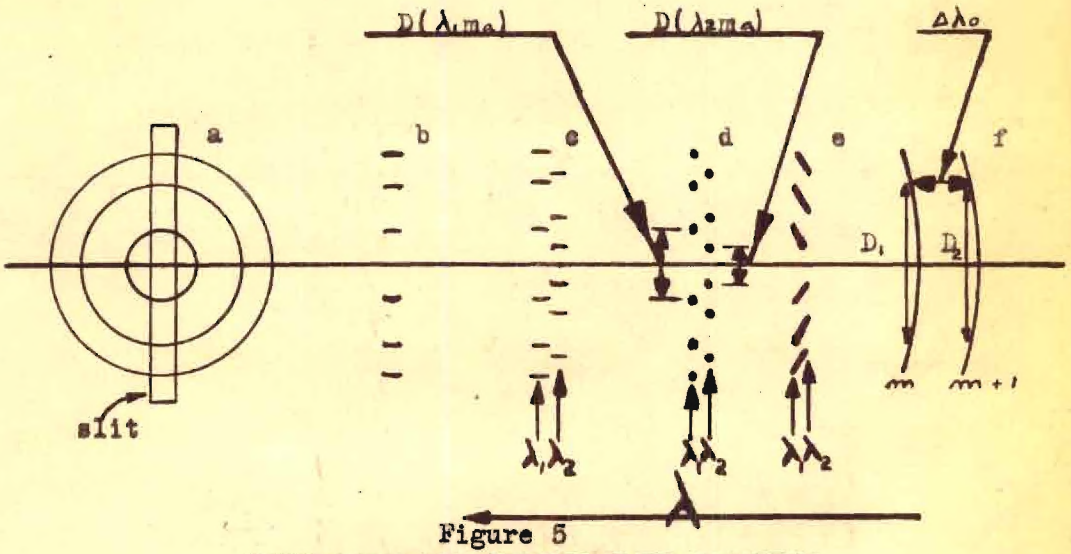

Figure 5

INTERFEROMETER-SPECTROGRAPH PATTERNS

See Text for Description

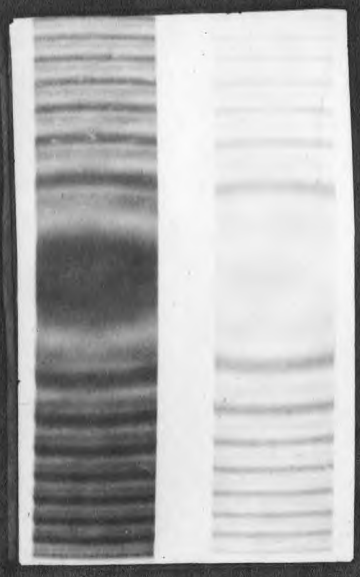

Figure 6

INTERFEROMETER-SPECTROGRAPH PATTERN FOR THE TWO YELLOW MERCURY LINES

The black arcs are sections of the fringe circles, since the figure is a negative print.

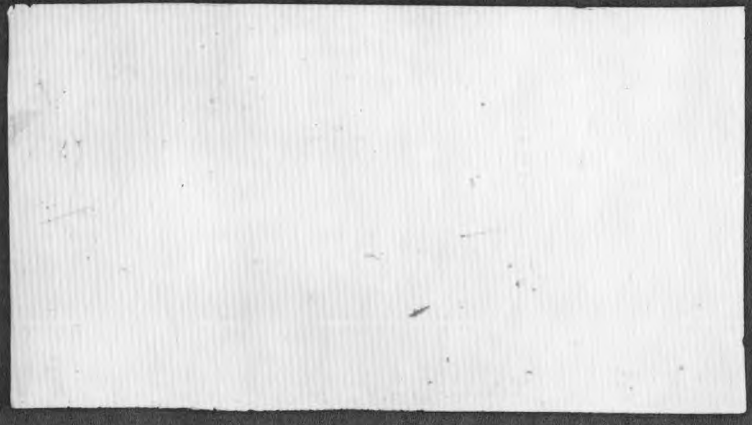

Figure 7

NEGATIVE PHOTOGRAPH OF A CHANNELLED SPECTRUM

The photograph was taken at 4,000 Å for an interferometer plate distance of 0.1576 cm. The apices of the parabolas do not appear on the spectrogram as a result of focusing the interference fringe centers below the spectrograph slit.

ring of some definite value of m and λ as calculated from Equation II, will decrease with λ. The relationship between D and λ is indicated in Figure 5d by the fact that $D(\lambda_2, m_a)$ is smaller than $D(\lambda_1, m_a)$, where λ_2 is smaller than λ_1. If the spectrum between λ_2 and λ_1 were continuous, the spectrogram would be similar to Figure 5e with points infinitely close together and hence consist of lines inclined to the dispersion of the spectrograph, Figure 7.

It is seen from Equation II that the pattern diagramed in Figure 5e is a section of a family of parabolas with apices on the axis of the center of the fringe pattern with one parabola for each value of m. For ordinary values of the constants t and f in Equation II, the parabolas appear to be almost vertical straight lines as shown in Figure 7. This pattern is known as a channelled spectrum.

It will be shown later that better absorption patterns are obtained on a channelled spectrum if the parabola lines touch. For infinitely sharp fringes, interference circles, the value of the slit width that will produce sufficiently broad parabola lines to yield a continuous background will be the distance along the dispersion between adjacent infinitely sharp parabola lines.

This distance may be considered constant for any two parabolas since the portions of the lines actually found on the spectrogram are essentially equi-distant. An expression for such a slit width may be derived in the following fashion.

From Equation II it is seen that the diameter D_1 of an interference fringe of order m for a wave length λ_1 will be equal to the diameter D_2 of a fringe of order $m + 1$ for λ_2 if

$$\lambda_1 m = (m+1)(\lambda_1 - \Delta\lambda_o), \quad \text{(III)}$$

where $\Delta\lambda_o = \lambda_1 - \lambda_2$. From Figure 5f it is seen that the difference in wave length corresponding to D_1 and D_2 is the difference between the wave length values for two adjacent parabolas, m and m + 1, and is, therefore, a measure of the slit width required to produce parabolas that touch. From Equations III and II, assuming $D^2/8f^2$ small, or from Equations III and I with cos θ equal to unity for small θ:

$$\Delta\lambda_o = \frac{\lambda_1}{m+1} = \frac{\lambda_2}{m} = \frac{\lambda_1\lambda_2}{2t} \quad \text{(IV)}$$

where $\Delta\lambda_o$ is the wave length between orders. Finally, the slit width for which the parabolas just touch for infinitely sharp fringes is seen to be:

$$\Delta s = \frac{\lambda_1 \lambda_2}{2\mp d} \qquad (V)$$

where d is the dispersion of the spectrograph in the region of λ_1 and λ_2.

In practice, however, the fringe thickness as well as the slit width contributes to the parabola line thickness. The relative influence of these two factors is indicated in the following discussion.

The points in Figure 5d are actually rectangles with a horizontal distance essentially equal to the slit width and a vertical dimension determined by the fringe thickness. Such rectangles are shown in Figure 8 as a portion of Figure 3 selected by a spectrographic slit where the horizontal and vertical dimensions represent the slit width and fringe thickness respectively. If λ_2 were increased so that the difference in λ_1 and λ_2 were equal to $\Delta\lambda_o$ in Equation IV, any rectangle for λ_2 in a given order would overlap that of λ_1 in the next highest order since the fringes would have the same diameter as indicated in Figure 9.

For five nearly equal wave lengths, with the difference in the longest and shortest wave length equal to $\Delta\lambda_o$, the pattern would become that diagramed in Figure 10 with the rectangles for λ_1 and λ_5 in adjacent orders overlapping. Further overlapping would occur if the source

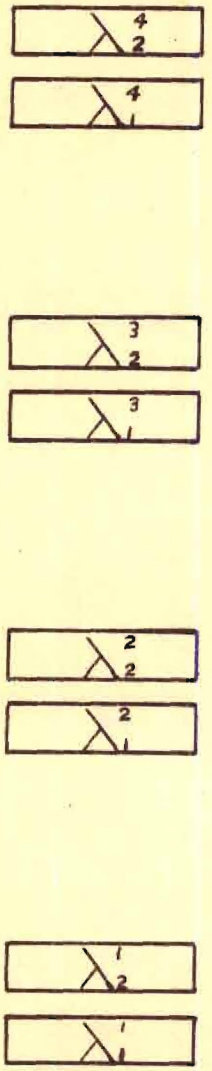

Figure 8

A PORTION OF FIGURE 3 SELECTED BY A SPECTROGRAPHIC SLIT

Figure 9

OVERLAPPING ORDERS FOR TWO WAVE LENGTHS

This figure illustrates the pattern that would exist for the two wave lengths in Fig. 10 if they differed by $\Delta \lambda_o$.

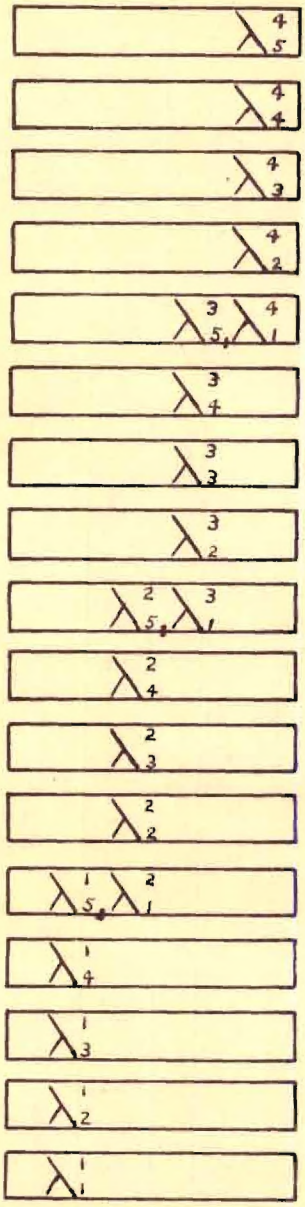

Figure 10

FRINGE PATTERN AT SLIT FOR FIVE NEARLY EQUAL WAVE LENGTHS WITH THE EXTREME VALUES DIFFERING BY $\Delta\lambda_0$.

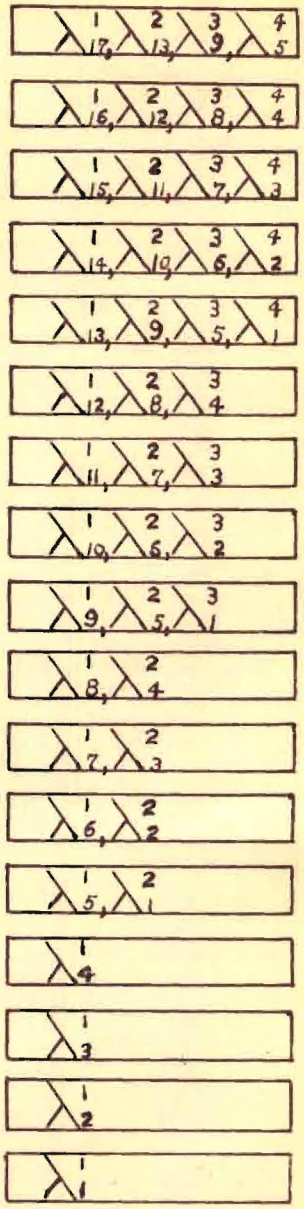

Figure 11

FRINGE PATTERN AT SLIT FOR SEVERAL NEARLY EQUAL WAVE LENGTHS WITH EVERY FIFTH DIFFERING BY $\Delta\lambda_0$.

contained wave lengths still greater than λ_5. For a sufficiently large number of wave lengths, rectangles for a given order may overlap those, several orders away. For example, λ_{10}^{1} would overlap λ_{2}^{2}, assuming equally-spaced wave lengths. Figure 11 illustrates, diagrammatically, the pattern obtained at the slit from a source consisting of a large number of frequencies, with the difference in every fifth wave length equal to $\Delta\lambda_o$. It is seen that the top five rectangles in Figure 11 represent four different wave lengths, each in a different order.

When the spectrograph disperses a pattern such as the top five rectangles in Figure 11, different wave lengths in a given rectangle are shifted along the dispersion of the spectrograph by different amounts, such that rectangles of the same order lie along the same parabola lines, as indicated in Figure 12. Note that overlapping rectangles differ by multiples of $\Delta\lambda_o$ and that this is the difference in wave length of adjacent parabolas as shown in Figure 5f. One of three possible interferometer-spectrograph patterns may result after dispersion by the spectrograph: non-touching, touching, and overlapping parabola segments. Figure 13 illustrates that either a broad slit or a thick fringe may cause either touching or overlapping parabolas.

If the difference in the wave lengths in Figure 12

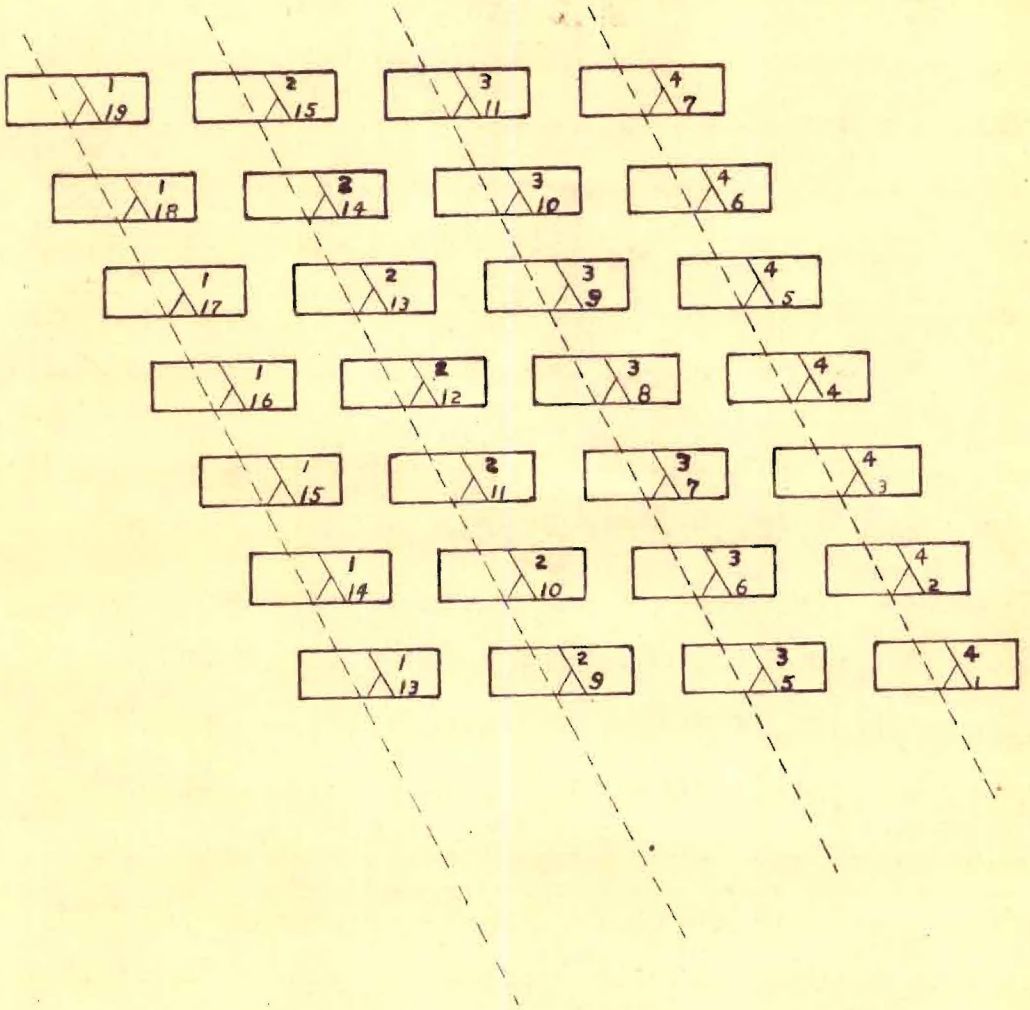

Figure 12

PATTERN GIVEN IN FIGURE 11 AFTER DISPERSION BY A SPECTROGRAPH

Dotted lines indicate parabolas

were infinitesimal, the rectangles on any one parabola would almost completely overlap to produce broad parabola segments with smooth sides similar to those sketched in Figure 14. Figure 14 is a diagram of several channelled spectra produced by a continuous light source. The hypothetical rectangles in the various illustrations have horizontal dimensions equal to various fractions $\Delta\lambda_o$, (See figure 5f) and vertical dimensions equal to various fractions of $\Delta D_o/2$, the vertical distance between neighboring parabolas.

The effect of slit width on the parabola thickness, for a given fringe thickness, is indicated in Figure 15 by the microphotometer traces of several channelled spectra, at about 4,000 Å, for several slit widths. Figures 15a and 15b are patterns for non-touching parabolas produced by a 0.05 mm and 0.08 mm slit, respectively. The greater density variation in Figure 15a is a result of a longer exposure time. The double maxima in Figure 15c indicate overlapping for a slit of 0.12 mm; whereas, at 0.18 mm, Figure 15d, the pattern is too complex for interpretation. The theoretical slit width for touching parabolas with zero fringes is calculated from Equation V to be about 0.1 mm, which seems to be in agreement with the observed values.

The slit width required by finite fringes to pro-

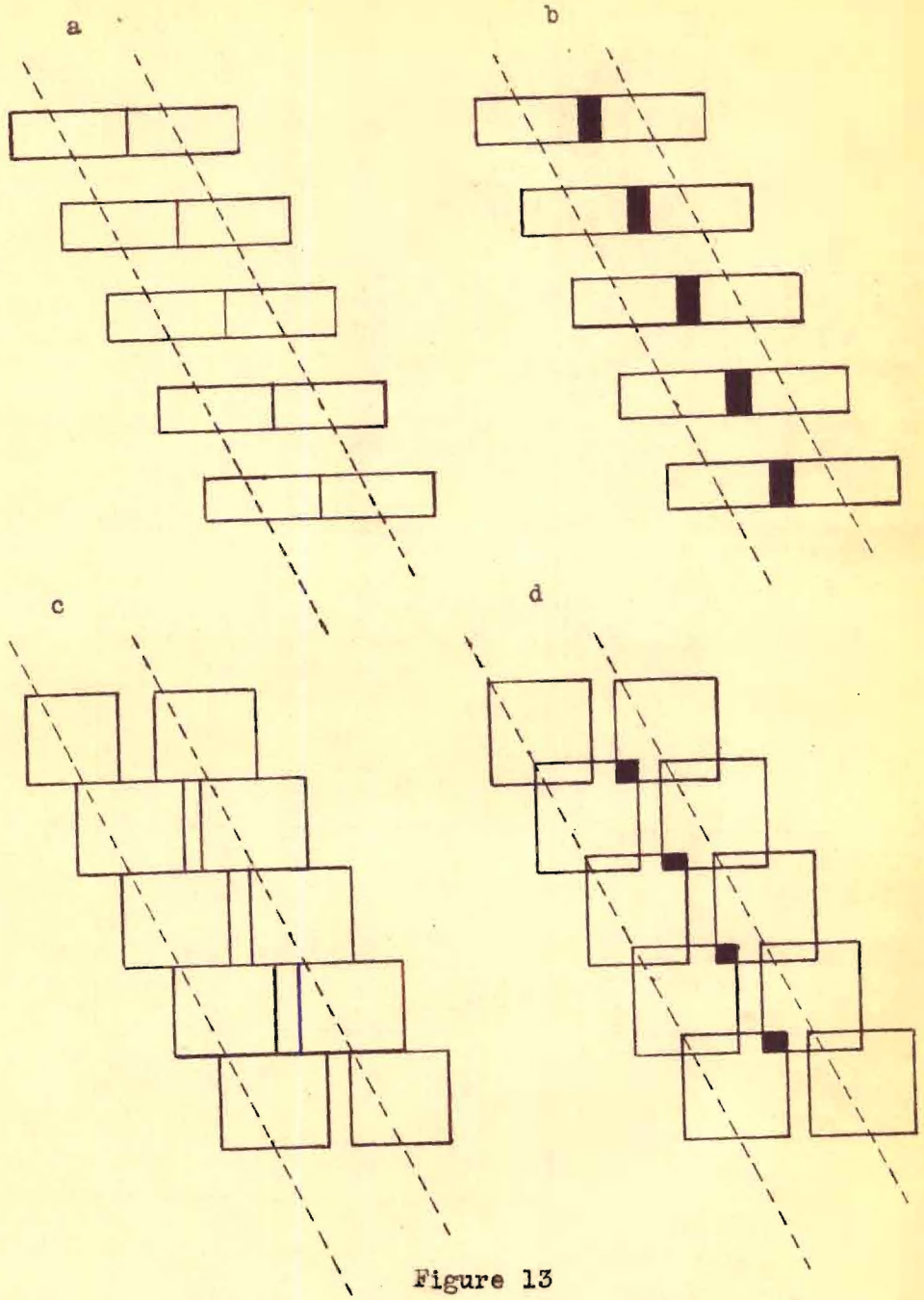

Figure 13

EFFECT OF SLIT WIDTH AND FRINGE THICKNESS

a. Touching parabolas due to wide slit, b. overlapping
c. Touching parabolas due to thick fringes, d. overlapping.
Blackened areas indicate overlapping, dotted lines indicate parabolas.

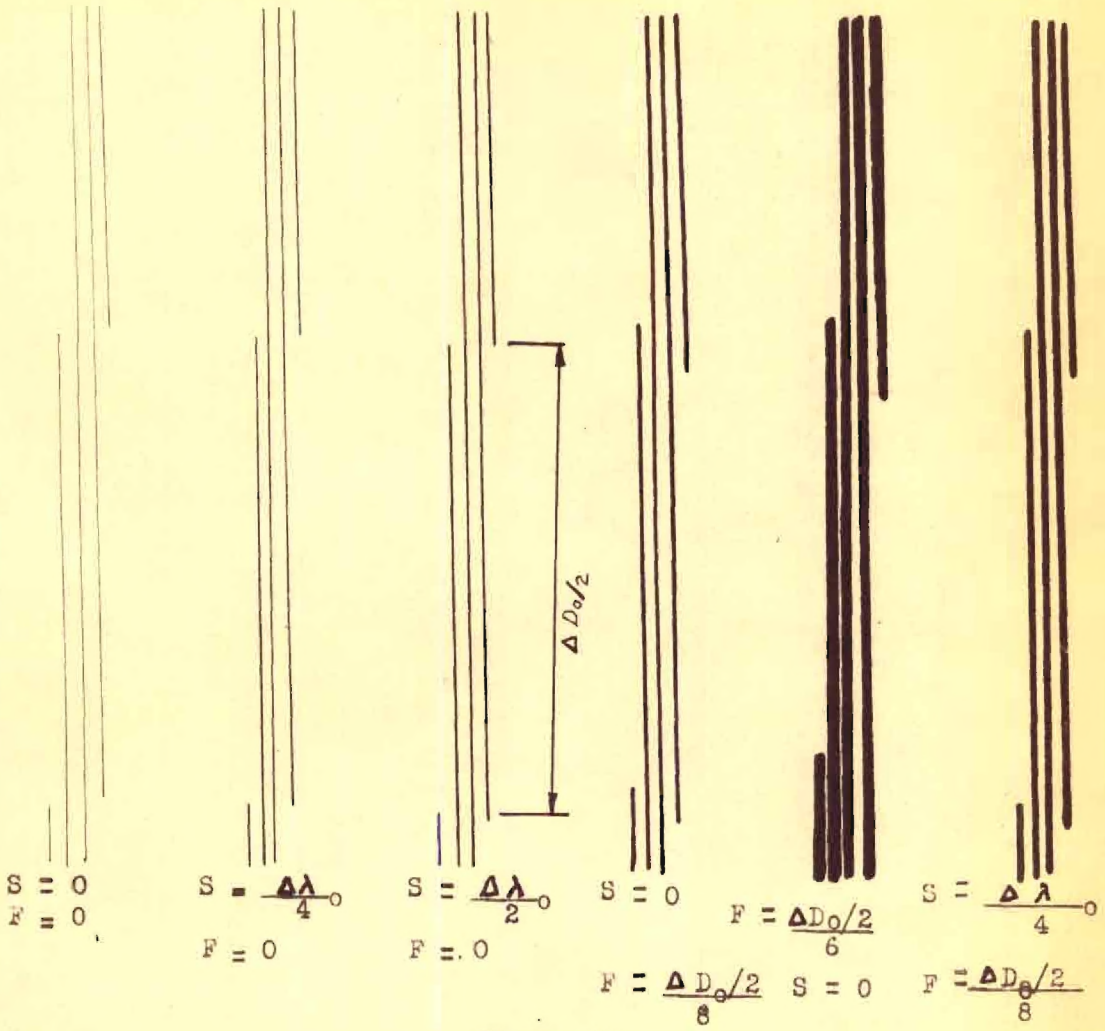

Figure 14

INTERFERENCE PATTERNS

S = Slit Width

F = Fringe Thickness

$D_o/2$ = Difference in radii of neighboring fringes of the same wave length.

$\Delta\lambda_o$, = Defined in Equation III

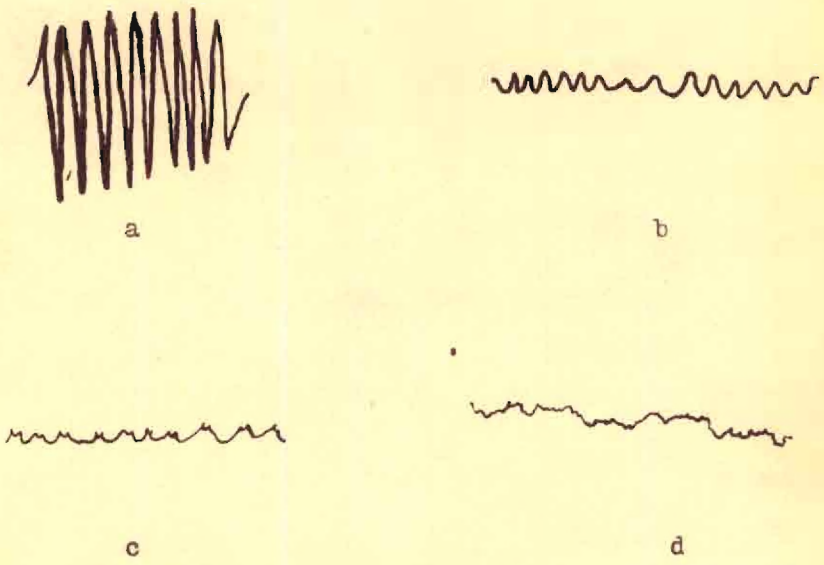

Figure 15

MICROPHOTOMETER TRACES OF CHANNELLED SPECTRA

Trace	Slit Width
a	0.03 mm
b	0.08 mm
c	0.13 mm
d	0.18 mm

See Text for Discussion of Traces

duce touching parabolas is clearly less than that defined by Equation V. For a given slit width, therefore, finite fringes require a greater spectrographic dispersion than that calculated from Equation V to produce touching parabolas. However, Equation V has a more serious limitation. When correctly adjusted to the condition of Equation V, the Bausch and Lomb Large Littrow Spectrograph will give a continuous background for a region of only about 500 Å at 4,000 Å, the limitation resulting from the variation of dispersion with wave length. The lines to shorter wave lengths do not touch; those to longer, overlap to give darker lines.

The mechanism by which greater resolution of absorption spectra is obtained with a channelled spectrum is indicated in Figure 16, which differs from Figure 12 only in the assumption that the slit width and the fringe thickness are such that all portions of adjacent parabolas touch. It is seen from Figure 16 that if the cross-sectioned rectangles (λ_9 and λ_{10}) were absorbed, the wave lengths of the absorbed rays could be determined by tracing along the vertical, dotted lines passing through the center of the rectangles to the wave length scale. The pattern of an ordinary spectrum could be obtained from Figure 16 by erasing all horizontal lines and extending all vertical lines. Clearly, λ_9 and λ_{10} would not be resolved in such a spectrogram.

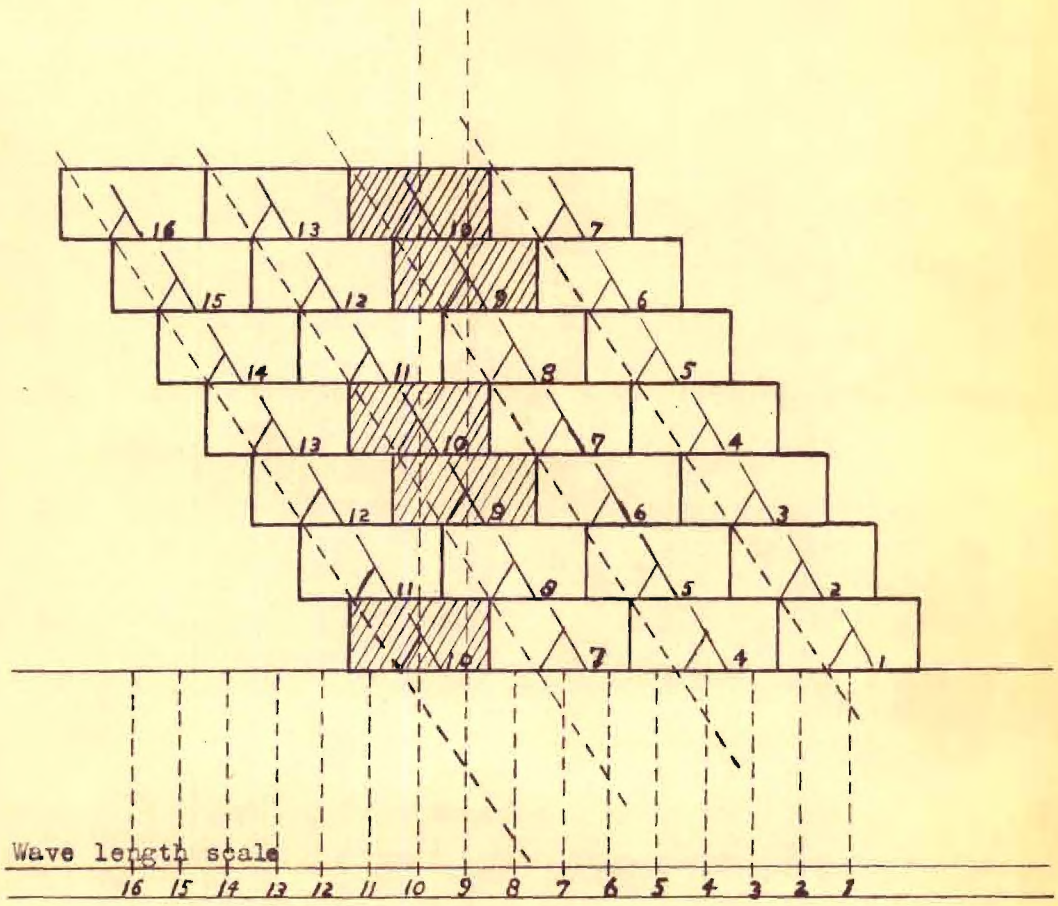

Figure 16

INTERFEROMETER - SPECTROGRAPH PATTERN
FOR A DISCRETE SOURCE

Pattern for a region of several nearly equal monochromatic rays with a slit width and fringe thickness such that all portions of adjacent parabolas touch. The inclined dotted lines represent the several parabolas formed by the corresponding blocks. The vertical dotted lines pass through the center of blocks of the wave length determined by the intersection of the dotted lines with the wave length scale.

If the parabola lines in Figure 16 did not touch, the absorption pattern would not be so clearly defined, since the spacing between the parabolas would tend to broaden the absorbed regions. However, it is seen from the following discussion that, for a certain type of measurement, it is desirable to take pictures of the absorption spectrum with non-touching parabolas.

An expression for the difference in the wave numbers of any two absorption features on the channelled spectrum may be obtained from Equation IV by setting $\Delta\lambda_0$ equal to $\Delta\tilde{\nu}\lambda_1 \lambda_2$, where $\Delta\tilde{\nu}$ is the difference in wave numbers, corresponding to λ_1 and λ_2, to obtain

$$\Delta\tilde{\nu} = \frac{\Delta m}{2t}. \qquad \text{(VI)}$$

If this is known, it is possible to determine $\Delta\tilde{\nu}$ quite accurately from a sufficiently enlarged spectrum with non-touching parabolas by counting the number of parabola lines, Δ m, between two absorption features.

The desirability of a thin fringe may be determined from a theoretical discussion of fringe thickness in terms of the reflection coefficient of interferometer plates. Tolansky[7] derives the following approximate formula

---

[7] S. Tolansky, High Resolution Spectroscopy (New York: Pitman Publishing Corporation, 1947) p. 104

from such a discussion:

$$d\nu = \frac{(0.98 - R)}{5t}, \quad 0.90 \geq R \geq 0.75, \quad \text{(VII)}$$

where $d\nu$, a measure of the fringe width, is the resolving limit in wave numbers, t is the distance between the interferometer plates, and R, the reflection coefficient of the plates, is the fraction of incident light reflected at the surface of an interferometer plate.

The value of R for a given interferometer may be estimated from plots given by Tolansky.[7] An indication of fringe thickness for several values of R is given in Figure 17, which is a plot of the intensity distribution of a given wave length from a point of maximum to a point of minimum intensity one half an order away. If a fringe differing in wave length by a tenth of an order appeared in Figure 17 with an intensity of 0.1, a reflection coefficient of at least 0.8 would be required before it could be distinguished well from the more intense neighboring line. From Equation VI, such a reflection coefficient corresponds to a fringe width of 0.24 cm^{-1} at the wave length of Figure 17, for a plate distance of 0.15 cm.

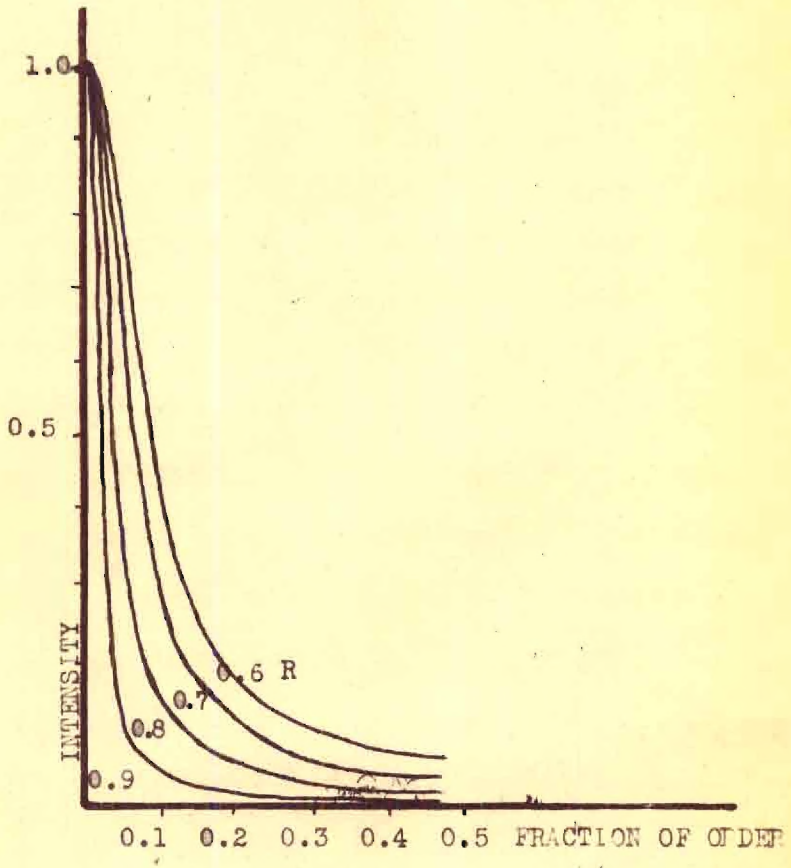

Figure 17

INTENSITY DISTRIBUTION FROM MAXIMUM INTENSITY POINTS FOR THE FABRY-PEROT INTERFEROMETER FOR A GIVEN FREQUENCY.

Taken from S. Tolansky, High Resolution Spectroscopy (New York, Chicago: Pitman Publishing Corporation, 1947) p.99.

VI

REQUIREMENTS ON THE SPECTROGRAPH

The theory developed in the previous section allows the precise specification of requirements on the spectrograph and associated properties of the interferometer.

As pointed out in the introduction, the principle limitation in the available apparatus lies in the resolution of the photographic plate. Assuming a resolving power of 50 lines per millimeter or 0.020 millimeters per line, the minimum usable slit width of the spectrograph should be about 0.025 millimeters.

For fringes of zero thickness, any assumed mimimum slit width that will produce a continuous background is related by Equation V to the interplate spacing and the corresponding maximum allowable spectrographic dispersion (Å/mm). This relation is indicated graphically in Figure 18 where the maximum dispersion, d_m, is plotted against the interferometer separation, t, for several wave lengths and a slit width of 0.025 millimeters. The dotted lines in the figure represent the dispersion of the Bausch

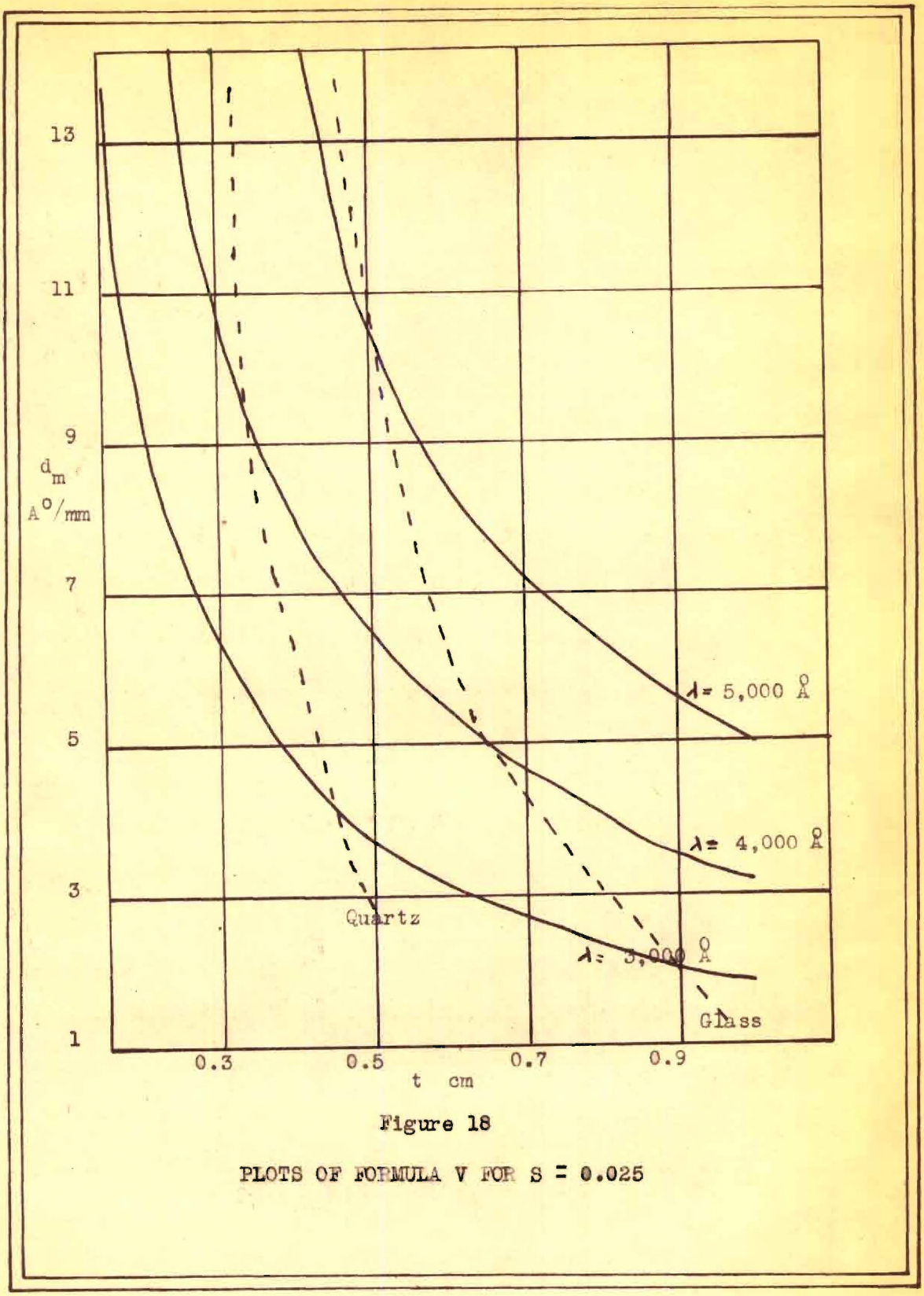

Figure 18

PLOTS OF FORMULA V FOR S = 0.025

and Lomb Large Littrow Spectrograph for both glass and quartz optics and define the region over which this instrument is applicable. Thus, the points in Figure 18 on or below the dotted lines specify values of t and λ for which an interferometer may be crossed with this instrument with a slit of 0.025 mm to produce respectively touching and non-touching parabolas for fringes of zero width.

It was pointed out in the previous section that, for a given slit width, fringes of finite width require a smaller dispersion than that determined by Equation V. Therefore, for the minimum slit width of 0.025 mm, finite fringes require a smaller maximum dispersion than that indicated in Figure 18. Consequently, those points on or slightly below the dotted lines in Figure 18 indicate t and λ values which are not applicable.

As indicated in Figure 18, any interferometer spacing less than the critical value will decrease the demands on the sharpness of the fringes and, from Equation V, will allow the use of wider slit widths and therefore, shorter exposure times. However, these gains are obtained only at the sacrifice of resolution as indicated by Equation VII and result in an increase in the planarity demanded of the interferometer surfaces.

In the present investigation, a spacing of 1/16 inch or 0.15 cm was chosen as optimising, at least approximately, these conditions. With this spacing, it was not possible to use the entire aperture of the interferometer, but only an area of about 5 mm in diameter, in order to obtain sharp fringes free from aberration. For such a spacing and with an assumed minimum reflection coefficient of 0.80, Equation V gives the slit width for touching parabolas at 4,000 Å as 0.1 mm and Equation VII gives the minimum resolving limit as 0.24 cm^{-1}.

With a focusing lens, L_2 in Figure 4, of 35 cm focal length, Equation II gives the approximate difference in radii of rings of successive orders near the center of the pattern as 0.10 mm and Equation IV gives the wave length interval between neighboring fringes as 0.5 Å. These values lead to a dispersion of the order of 0.5 Å/mm normal to the dispersion axis of the spectrograph and a theoretical resolution of about 0.04 Å.

VII

PARABOLA BROADENING DUE TO TEMPERATURE AND PRESSURE CHANGES

For accurate control of parabola thickness, it is necessary to consider the vertical and horizontal broadening due to temperature and pressure changes. The change in the refractive index of air and the expansion of the plate spacers in the interferometer during exposure time will produce broadening in both the horizontal and vertical directions; the expansion of the coating on the surface of the interferometer plates will produce vertical broadening.

Table I lists equations for the distance broadening on the photographic plate in terms of temperature and pressure changes. The equations in the second and third columns are respectively for the distance broadening in the vertical direction, ΔV, and horizontal direction, ΔH, and those in the fourth column represent the horizontal component due to the increase in the vertical distance between the edges of the parabolas, ΔH_V. The sum of the two horizontal effects is the total broadening

along the axis of the dispersion of the spectrograph.

The equations in Table II express values of the fractional broadening of the distance between neighboring parabolas; the second column for the fraction of the vertical distance, $f\,\Delta D_o/2$; the third and fourth columns for the fraction of the horizontal distance, $f\,\Delta S_o$, due to ΔH, and ΔH_v, respectively. The equations in Tables I and II are evaluated in terms of temperature and pressure changes in Tables III and IV respectively where values assumed for the various constants are indicated in the tables. The derivation of these equations is discussed in the following sections of this chapter.

The following discussion of broadening due to the expansion of the plate coating material is necessarily made for silver since little data exists for other substances. Even though the plates used in this work were coated with aluminum, this discussion should be useful in determining the order of magnitude of the broadening as well as the data necessary for such a study.

All equations in Tables I and II are expressed in terms of temperature or pressure changes with the exception of the equations for the expansion of the coating material. The change in reflection coefficient, ΔR, in these equations may be determined from the temperature change

TABLE I

DISTANCE BROADENING OF PARABOLAS DUE TO TEMPERATURE AND PRESSURE CHANGES

Cause of Broadening	Vertical ΔV	Horizontal, ΔH	Horizontal Component of Vertical, ΔH_V
Refractive Index	$\frac{2(n)(n-1)M\rho f^{*}}{RT^{2}D}$	$\frac{n(n-1)M\rho\lambda^{*}}{RT^{2}d}$	$\frac{n(n-1)M\rho\lambda^{*}}{RT^{2}}$
Expansion of Spacers	$\frac{2\alpha f^{2}}{D}\Delta T$	$\frac{\alpha\lambda}{d}\Delta T$	$\alpha\lambda\Delta T$
Expansion of Coating Material	$\frac{2\lambda f^{2}}{5Dt}$ ΔR**	----------	$\frac{\lambda^{2}}{5t}$ ΔR**

*Times the quantity: $(\rho\Delta T - T\Delta\rho)$

**See Page 39

TABLE II

FRACTIONAL BROADENING OF PARABOLAS DUE TO TEMPERATURE AND PRESSURE CHANGES

Cause of Broadening	Vertical, $f\,\Delta D_o/2$	Horizontal, $f\,\Delta S_o$ Due to ΔH	Horizontal, $f\,\Delta S_o$ Due to ΔH_v
Refractive Index	$\frac{2n(n-1)M\rho t^*}{\lambda RT^2}$	$\frac{2n(n-1)M\rho t^*}{\lambda RT^2}$	$\frac{2n(n-1)M\rho dt^*}{\lambda RT^2}$
Expansion of Spacers	$\frac{2t\alpha\,\Delta T}{\lambda}$	$\frac{2t\alpha\,\Delta T}{\lambda}$	$\frac{2dt\alpha\,\Delta T}{\lambda}$
Expansion of Coating Material	$\frac{2}{5}\,\Delta R^{**}$	----------	$\frac{2d}{5}\,\Delta R^{**}$

* times the quantity: $(P\,\Delta T - T\,\Delta P)$

** See page 39

TABLE III

VALUES OF FORMULAS IN TABLE I FOR CONDITIONS OF THIS WORK

Cause of Broadening	Vertical, ΔV	Horizontal, ΔH	Horizontal Component of Vertical, ΔH_v
Refractive Index	For P = 0, 4×10^{-3} ΔT mm/°K For T = 0 7×10^{-3} ΔP mm/mm Hg	For P = 0 7×10^{-4} ΔT mm/°K For T = 0 3×10^{-4} ΔP mm/mm Hg	For P = 0 4×10^{-11} ΔT mm/°K For T = 0 1×10^{-11} ΔP mm/mm Hg
Expansion of Spacers	1×10^{-4} ΔT mm/°K	1×10^{-2} ΔT mm/°K	5×10^{-10} ΔT mm/°K
Expansion of Coating Material	*	----------	*

*Neglible, See page 39

P, 1 at; λ, 4,000Å; d, 5 Å/mm; α (Ag), 1.9×10^{-5}/°K; f, 35 cm; T, 300 °K; t, 0.15 cm., α (steel), 1.3×10^{-5} /°K; D, 3.5 cm., $t' = 40 m\mu$

TABLE IV

VALUES OF EQUATIONS IN TABLE II FOR CONDITIONS OF THIS WORK

Cause of Broadening	Vertical, $\Delta D_o/2$	Horizontal, $f\Delta S_o$ Due to ΔH	Horizontal, $f\Delta S_o$, Due to ΔH_v
Refractive Index	For P=0, $7 \times 10^{-3}\ \Delta T$ mm/°K For T 0, $3 \times 10^{-4}\ \Delta P$ mm/mm Hg	For P=0, $7 \times 10^{-3}\ \Delta T$ mm/°K For $3 \times 10^{-4}\ \Delta P$ mm/mm Hg	For P=0, $4 \times 10^{-10}\ \Delta T$ mm/°K For T=0, $1 \times 10^{-10}\ \Delta P$ mm/mm Hg
Expansion of Spacers	$0.1\ \Delta T$ mm/°K	$0.1\ \Delta T$ mm/°K	$5 \times 10^{-9}\ \Delta T$ mm/°K
Expansion of Coating Material	*	----------	*

*Negligible: See Page 39

P, ⊥ at: λ, 4,000Å; d, 5 Å/mm; α (Ag), 1.0×10^{-5}/°K; f, 35 cm; T, 300 °K; t, 0.15 cm.; α(steel), $1/3 \times 10^{-5}$/°K; D, 3.5 cm., $t' = 40\ m\mu$

of a silver coating material, ΔT, by use of the Fabry equation[8, 2] and an empirical chart by Fizeau[9, 2]. The Fabry equation

$$D' = 0.035\ t' \qquad \text{(VIII)}$$

where D' is the optical density of the plate and t' is the thickness of the coating material in millimicrons, may be expressed as

$$\Delta D' = 0.035\ t' \alpha\ \Delta T \qquad \text{(IX)}$$

where $\Delta D'$ is the change in optical density due to a change in temperature ΔT, and α is the linear coefficient of expansion for silver. It is then possible to determine ΔR from Fizeau's chart, Figure 19, for use in the equations in Tables I and II by calculation of D' and $\Delta D'$ from Equations VIII and IX.

In the following derivation of the equations in Tables I and II, three equations are first derived for $\Delta \lambda_\mu$, the change in wave length due to refractive index change $\Delta \lambda_s$, and $\Delta \lambda_c$, the wave length shift in the instruments due to expansion of the spacers and coating.

---

[8] Fabry, Les Applications des Interferences Lumineuses (1927)

[9] Fizeau, Annales de Chimie et de Physique, 63, 393 (1861)

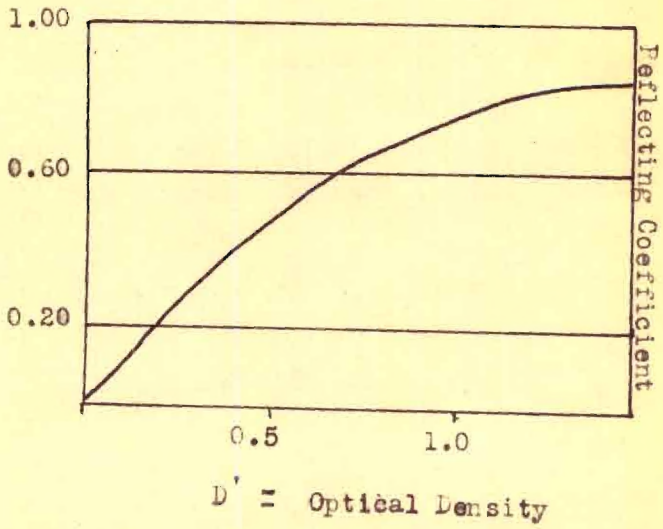

Figure 19

REFLECTION COEFFICIENT FOR SILVER COATING

Taken from: Fizeau, Ann. de Chim et de Phys., 63, 393. 1861.

The change in wave length due to refractive index change, $\Delta\lambda_n$, may be determined in the following manner. Since

$$\begin{aligned} \lambda &= k'/n, \text{ for a given frequency} \\ n-1 &= k''\rho, \text{ and} \\ \rho &= PM/RT, \text{ for an ideal gas,} \end{aligned}$$

where n is the index of refraction of air, λ is the wave length in air k' and k'' are constants, ρ is the density of air, and P,T, and M are the pressure, temperature, and molecular weight of air, it is seen that

$$\lambda = \frac{k'T}{\frac{k''PM}{R}} \cdot \frac{1}{T}$$

Upon differentiation, the following are obtained:

$$\left(\frac{\delta\lambda}{\delta T}\right) = \frac{k'k''MP}{RT^2},$$

$$\left(\frac{\delta\lambda}{\delta P}\right) = \frac{-k'k''M}{RT},$$

where the quantity $Pk''M/R = (n-1)T$ is considered negligible. For example, for a wave length of 4,000 Å in air at 15°C and one atmosphere of pressure, $Pk''M/R$ is equal to 8.11×10^{-2}°K. Finally, it is seen that

$$d\lambda = \left(\frac{\delta\lambda}{\delta P}\right)dP + \left(\frac{\delta\lambda}{\delta T}\right)dT = \frac{k'k''M}{RT^2}(PdT - TdP), \text{ or}$$

$$\Delta\lambda_n = \frac{n(n-1)M\rho\lambda}{RT^2}(P\Delta T - T\Delta P) \qquad (X)$$

If the fringe thickness, $\Delta \tilde{\nu}$, is defined by Equation VI, the change of fringe thickness $\Delta\lambda_t$, due to the expansion of the plate coating is given by

$$\Delta\lambda_t = \frac{\lambda^2}{5t} \Delta R \qquad \text{(XI)}$$

where $\Delta\lambda_t$ is set equal to $(\partial\tilde{\nu}_2 - d\tilde{\nu}_1)(\lambda^2)$, and where ΔR is the change in reflection coefficient due to the expansion of the plate coating. Finally, an expression for the broadening due to the expansion of the spacers, $\Delta\lambda_s$, is seen from Equations IV and I to be:

$$\Delta\lambda_s = \frac{\lambda}{t} \Delta t = \lambda \alpha \Delta T \qquad \text{(XII)}$$

where cos θ is considered unity, and where Δt is the change in plate spacing due to the temperature change ΔT producing $\Delta\lambda_s$, and α is the linear coefficient of expansion of the spacers.

The two equations in Table I for horizontal broadening, ΔH, are obtained by expressing λ_r and λ_τ in terms of the spectrographic dispersion. The remaining equations in Table I are obtained in the following fashion.

Upon rearrangement and differentiation of Equation II and appropriate substitution of Equation I with cos θ equal to unity it is seen that

$$\left(\frac{\delta D/2}{\delta \lambda}\right) = \frac{f^2 m}{tD} \approx \frac{2f^2}{\lambda D}, \quad \text{and} \qquad \text{(XII)}$$

$$\left(\frac{\delta D/2}{\delta m}\right) = \frac{f^2 \lambda}{tD} \qquad \text{(XIV)}$$

since m changes continuously if λ is not constant. Therefore,

$$dD/2 = \left(\frac{\delta D/2}{\delta \lambda}\right) d\lambda + \left(\frac{\delta D/2}{\delta m}\right) dm = \frac{f^2}{D} (2/\lambda \; d\lambda + \lambda/t \; dm).$$

or

$$\Delta V = \Delta D/2 = \frac{f^2}{D} (2/\lambda \; \Delta\lambda + \lambda/t \; \Delta m) \qquad \text{(XV)}$$

where ΔV is the change in the vertical dimension of a parabola.

The three equations in Table I for ΔV are obtained from Equation XV by setting Δm equal to zero since only one parabola is under consideration and by placing $\Delta\lambda$ equal to the $\Delta\lambda$ values derived above for each of the three effects contributing to parabola broadening. If the equations for ΔV are divided by the slope of the parabola, Equation XIII, the equations in Table I for ΔH_V result, the fractional broadening equations in Table I by $\Delta D_o/2$ for vertical broadening and by ΔS_o for horizontal broadening. These values are obtained in the following manner.

The horizontal distance between parabolas, ΔS_o, is

the value of the slit width required to produce touching parabolas for fringes of zero width. This is the quantity ΔS given in Equation V. The value $\Delta D_o/2$, the vertical distance between parabolas, is the distance between successive fringes of the same wave length. Setting $\Delta\lambda$ equal to zero and Δm equal to unity in Equation XI, we have

$$\Delta D_o/2 = \frac{\lambda f^2}{tD} \qquad (XV)$$

From Table III it is seen that a temperature change of one degree will produce a broadening of approximately 0.01 mm along the dispersion of the spectrograph, and a pressure change of 30 mm Hg is required to produce the same effect. Vertical broadening will occur to this extent for temperature and pressure changes of three degrees and two millimeters of mercury, respectively. Since, as pointed out in the previous section, the maximum resolution of the plate is about 0.02 mm, temperature changes of 4°C and pressure changes of 8 mm of Hg should be barely noticeable.

VIII

EXPERIMENTAL MEASUREMENTS ON THE ABSORPTION SPECTRUM OF NO_2

The following considerations were the factors which led to the choice of NO_2 for absorption measurements in this study: 1) NO_2 has considerable structure in the region in which greater resolution is needed, i.e., 4,000 Å.; 2) A short absorption cell, 10 cm., low pressures, 15 mm., and room temperature are suitable conditions for absorption in this region; 3) NO_2 is easily prepared with sufficient purity, and is sufficiently stable, to produce a dependable absorption spectrum; 4) No diatomic molecule could be found with a sufficient number of the above advantages to permit its use with the available equipment.

NO_2 was prepared by heating a mixture of sand and lead nitrate and distilling the gas through a side arm into the cell which was placed in a methyl alcohol-dry ice bath. The cell was then alternately slightly warmed and evacuated to remove all foreign gaseous material along with some NO_2. Finally, the cell was closed and

warmed to room temperature. The final pressure was obtained by partial evacuation to a pale yellow color.

The optical path for this work was essentially that outlined in Figure 4. The light source was a 100 watt incandescent bulb mounted in front of a focusing mirror to conserve light. Economy of light was somewhat necessary since considerable reduction in intensity resulted from reflection at the first plate of the interferometer. An iris diaphragm in the source mounting projected the beam on the end of the absorption cell which followed immediately. The cylindrical cell was 10 cm in length and 1.5 cm in diameter with pyrex glass windows. A stopcock was connected to the side of the cell to permit filling. The light then passed through a 50 cm focal length converging lens, L_1 in Figure 4, to concentrate the beam on the first interferometer plate in an area of about 5 mm in diameter as discussed in the previous section. A 35 mm focal length high quality achromatic lens, L_2 in Figure 4, focused the light transmitted by the interferometer on the spectrographic slit. Several exposures were taken with a mercury lamp source to determine the optimum position of L_2 for the ultra-violet.

Since it was found desirable to focus the center of the fringe pattern above or below the slit to obtain both sharper fringes and more nearly linear parabola lines,

the interferometer was mounted on a base which could be rotated about a horizontal axis and accurately adjusted to the desired position by a screw mechanism. Type 103-F3 plates with a resolving power of 45 lines per millimeter were used. This required an exposure time of about four hours for a channelled spectrum and a slit of 0.08 mm and about thirty minutes for no interferometer and a slit of 0.03 mm.

The first measurement made on the channelled spectrum was similar to that described in connection with Equation VII. However, the purpose here was to determine the value of the interferometer spacing t from a known value of $\Delta\tilde{\nu}$. A double exposure of a channelled spectrum, with no absorption cell, and an iron arc covering only a portion of the channelled spectrum was used for this measurement. The partially overlapping iron lines facilitated the exact determination of the region over which the parabola lines were counted. The number of parabola lines, Δm, were counted on a projection of the plate (enlarged by a factor of 15) between two iron lines of known wave length, λ_1 and λ_2. The wave numbers from which $\Delta\tilde{\nu}$ was calculated were obtained from Kayser's Tables[10] which are corrected for the refractive index

[10] H. Kayser, Tabelle der Schwingungszahlen (Ann Arbor, Michigan: Edward Brothers, Inc., 1944)

of air. Various values of λ_1, λ_2, Δm, and t are listed in Table V. The average of the experimental quantities indicate a value of the plate distance of 0.15760 cm $\pm$ 0.00003 cm.

Figures 20 and 21 present enlargements of a spectrogram showing a millimeter scale, an iron arc spectrum, a channelled absorption spectrum and an ordinary absorption spectrum of NO_2 in the region of 4,000 Å. A general comparison of the two absorption spectra will reveal the fact that greater structure can be seen in the channelled spectrum. However, the very thin parabola segments, visible in these figures, should not be confused with NO_2 structure. The ink dots in the figures indicate some of the more obvious cases of increased resolution. Figure 22 shows bands at 108 and 112.5 with greater contrast.

Values of Δm between various absorption features and the iron line at 22,587 cm^{-1} were determined in the region between 104 and 112 on the scale in Figures 20 and 21 to yield differences in wave numbers, $\Delta\tilde{\nu}$. The values of $\Delta\tilde{\nu}$ were appropriately added and subtracted from 22,587 cm^{-1} to obtain the wave numbers of the various absorption features. Various values of Δm, $\Delta\tilde{\nu}$, and the final wave numbers are recorded in Table VI. The last column in this table indicates the corresponding conditions in the ordinary spectrum.

TABLE V

DETERMINATION OF THE INTERFEROMETER PLATE DISTANCE

λ_1 °	λ_2 °	Δm	t
4,315.09 A	4,225.46 A	155.0	0.1577 cm
4,315.09	4,430.62	190.5	0.1576
4,602.95	4,442.35	247.5	0.1576

Average: $t = 0.15760$ cm $\pm$ 0.00003 cm

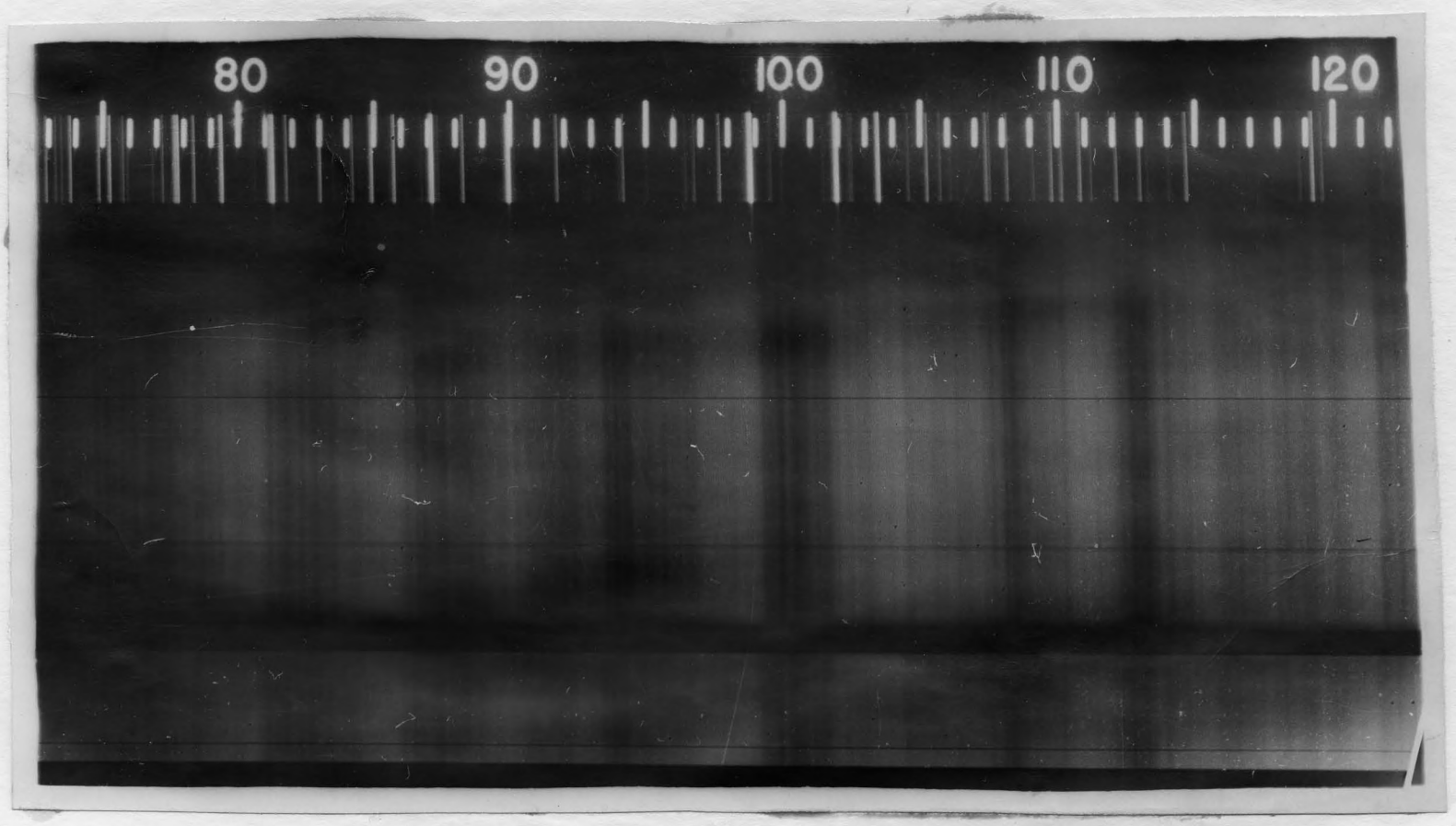

Figure 20

POSITIVE PHOTOGRAPH OF A CHANNELLED AND ORDINARY ABSORPTION SPECTRUM OF NO_2

a. channelled, b. ordinary

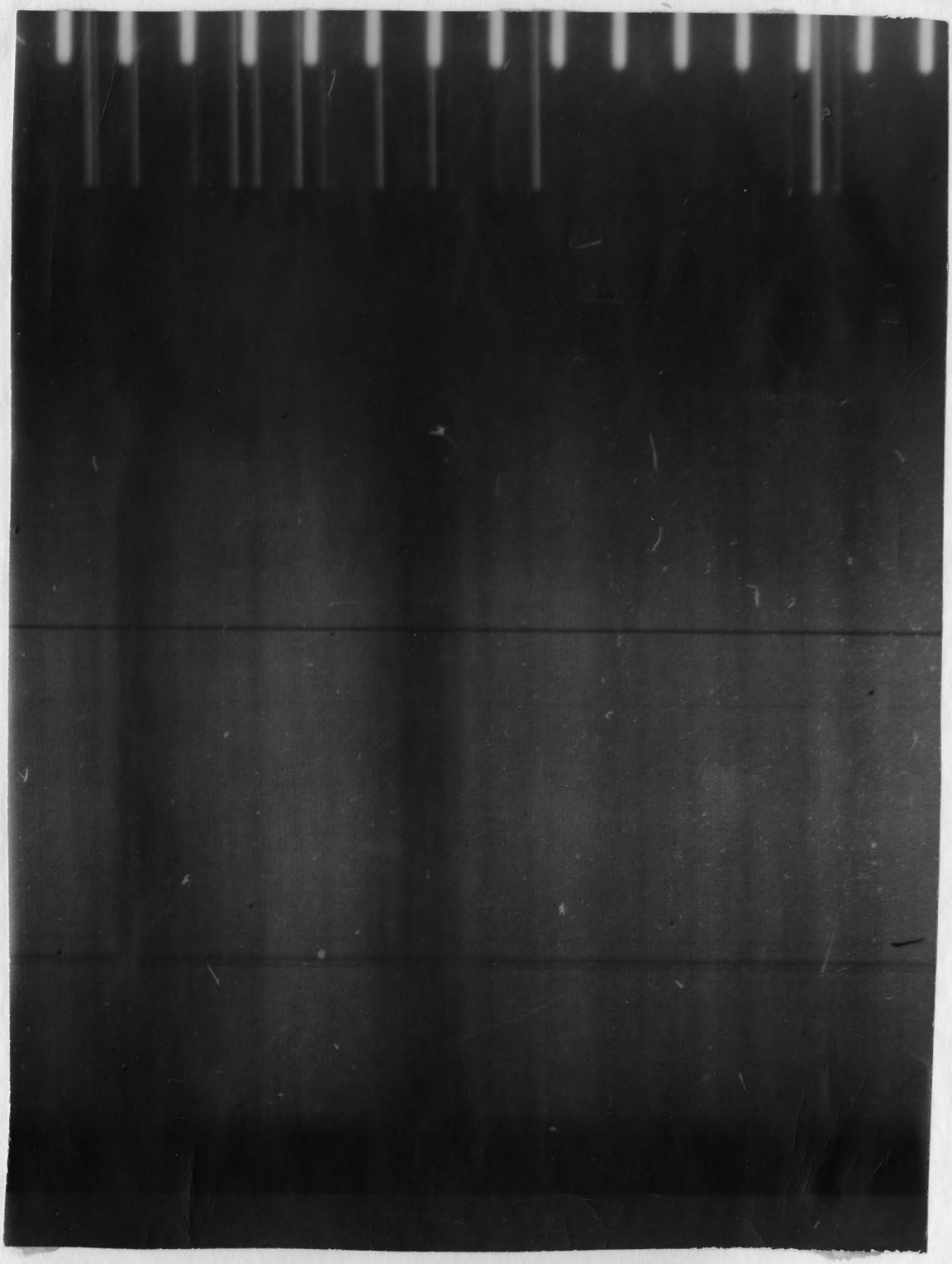

Figure 21

POSITIVE ENLARGEMENT OF FIGURE 20

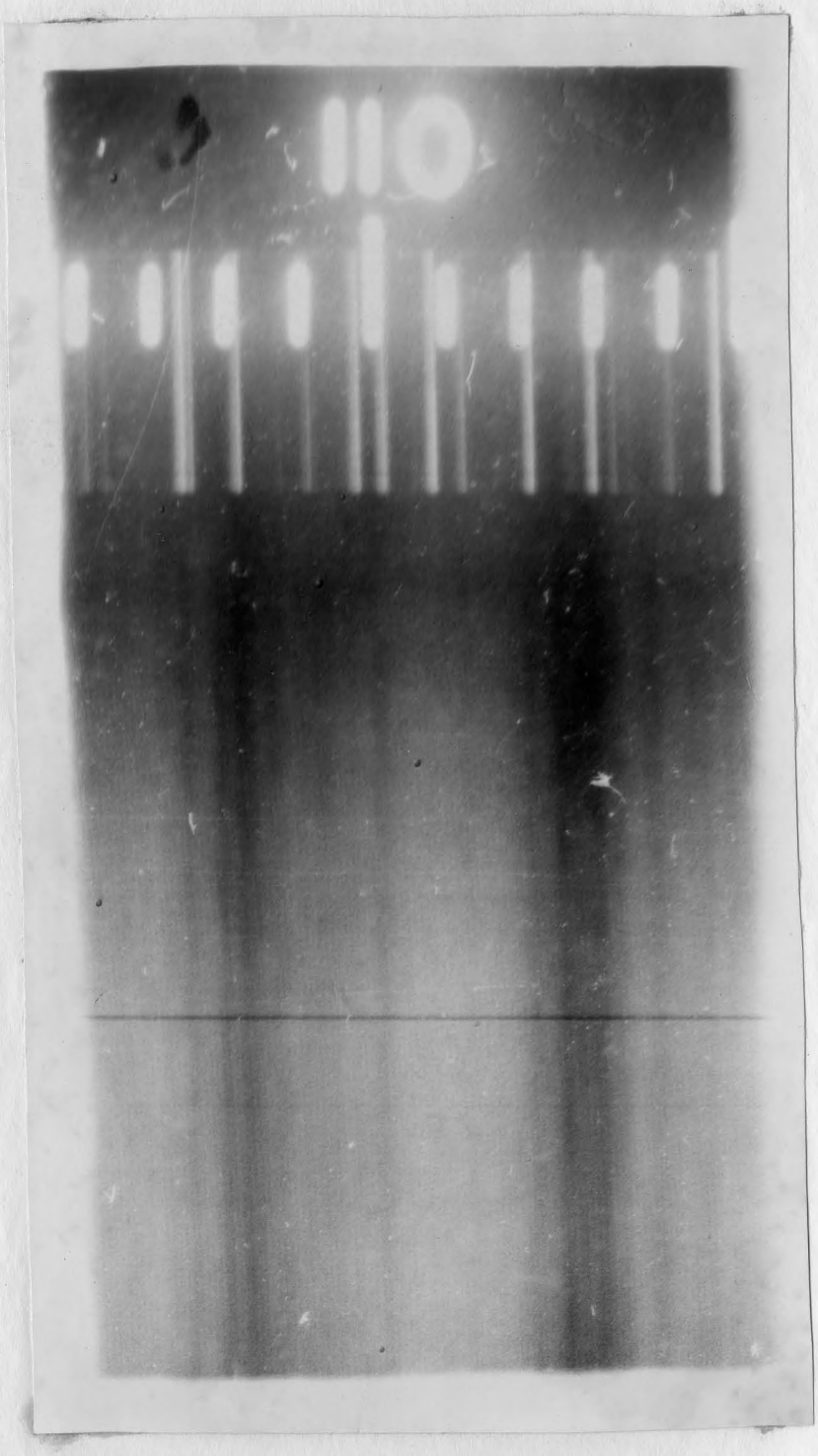

Figure 22

POSITIVE PHOTOGRAPH OF BANDS AT 108 AND 112.5 IN FIGURE 20

TABLE VI

BANDS OBSERVED IN REGION OF 104 to 112
IN FIGURES 20 AND 21

Δm	$\Delta \tilde{\nu}$	$\tilde{\nu}$	Ordinary Spectrum
+12.0	38.0	22,625.0	
+9.0 R	29.0	616.0	B. R.
+1.0 R	3.0	590.0	B. R.
-8.5	27.0	560.0	B. R.
-20.0	64.0	523.0	B. D.
-25.0	80.0	507.0	B. D.
-31.5 I	100.0	487.0	B. D
-33.5 I	107.0	480.0	B. D
-37.5 mI	119.0	468.0	
-40.5 B & D	129.0	458.0	
-44.0	139.0	448.0	B. D.
-48.0	152.5	435.5	
-52.5 mI	167.0	420.0	
-56.5	179.5	408.5	
-58.0	184.5	403.5	D.
-60.0	190.0	397.0	B. D.
-63.0	200.00	387.0	
-65.5	208.5	379.5	D.
-73.5	233.0	354.0	D.

Con't.

TABLE VI - Con't.

Δm	$\Delta \tilde{\nu}$	$\tilde{\nu}$	Ordinary Spectrum
-79.5 mI	252.0	335.0	
-80.5 I	255.5	332.5	D
-83.5 I	265.5	322.5	
-86.0 I	274.5	313.5	D

Values of Δm are measured from the 22,587 cm^{-1} iron arc and are accurate to only 0.5.

I, Intense mI Medium Intensity

B, Broad D, Diffuse

R, Shaded to Red

From the absorption spectrum of NO_2 in the region of 4,000 Å certain bands were selected as those resulting from a transition from the lowest vibrational level in the ground electronic state. These bands were selected as a result of an estimation of their spacing, allowing for perturbations, determined from estimated vibrational frequencies of the upper electronic state, and from their greater intensities. Since NO_2 is an odd molecule, these absorption bands appear as doublets.

The approximate wave numbers of the doublets selected are listed in Table VII and plotted against a running index in Figure 23. The nature of these curves does indeed indicate that these bands might well belong to a vibrational sequence. Table VIII lists the difference in the wave numbers of the doublets as determined both by Equation VI and a Hartmann equation, where the wave lengths were converted to wave numbers by use of Kayser's Tables[10]. These differences are plotted against a running index in Figure 24 where the greater accuracy of Equation VI is indicated by the fact that the data in Figure 24a fit a smooth curve much more closely than those in Figure 24b.

The channelled spectrum has made possible both the measurement of more absorption lines and a more ac-

TABLE VII

DOUBLET COMPONENTS SELECTED FROM THE ABSORPTION SPECTRUM OF NO_2

Wave Numbers	Wave Numbers
23,720	23,690
23,550	23,520
23,400	23,360
23,210	23,180
22,970	22,940
22,770	22,730
22,450	22,430
22,300	22,270
21,980	21,950
21,600	21,580
21,060	21,040
20,480	20,440
19,870	19,830
19,220	19,190

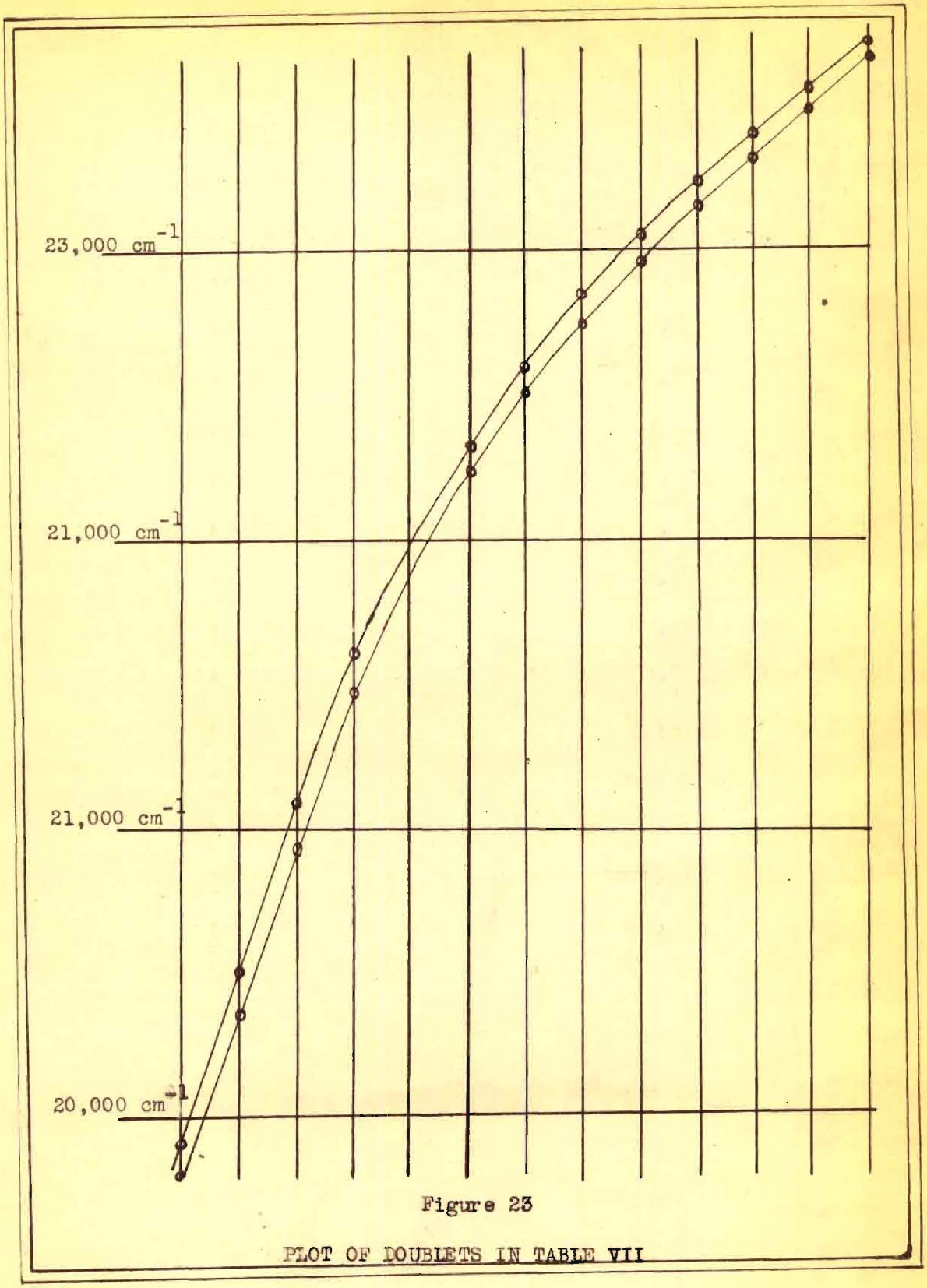

Figure 23

PLOT OF DOUBLETS IN TABLE VII

TABLE VIII

DIFFERENCE IN WAVE NUMBERS OF DOUBLET COMPONENTS IN THE ABSORPTION SPECTRUM OF NO_2

Δ m	$\Delta \tilde{\nu}$ by Equation VI	$\Delta \tilde{\nu}$ by Hartmann Equation
16.0	50.8	34.8
16.5	52.4	49.6
18.0	57.1	54.2
16.5	52.4	44.1
17.0	54.0	46.8
15.5	49.2	38.9
15.5	49.2	48.0
16.0	50.8	36.3
16.5	52.4	57.2
16.5	52.4	60.5
16.0	50.8	63.1
18.0	57.1	49.2
21.0	66.7	43.5
20.0	63.5	49.2

Values of Δ m are accurate to only 0.5

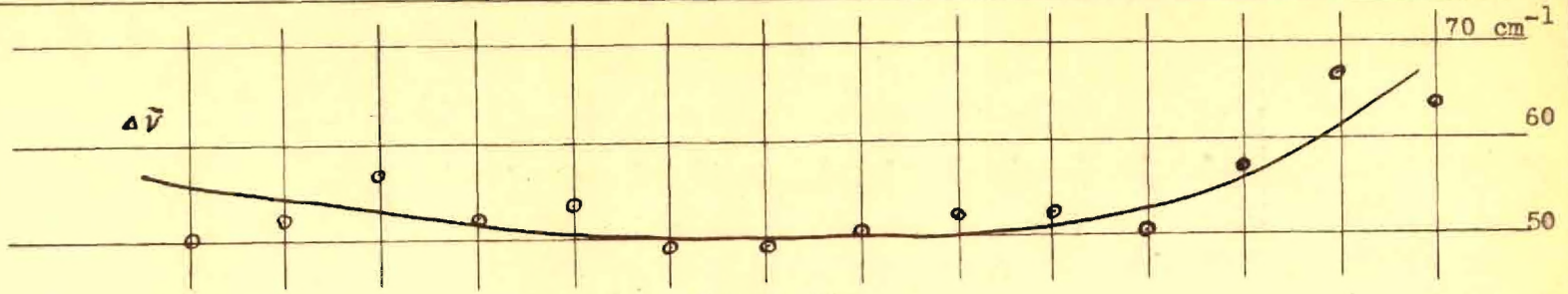

Figure 24a

DOUBLET SEPARATION OF NO_2 BANDS
BY EQUATION VI

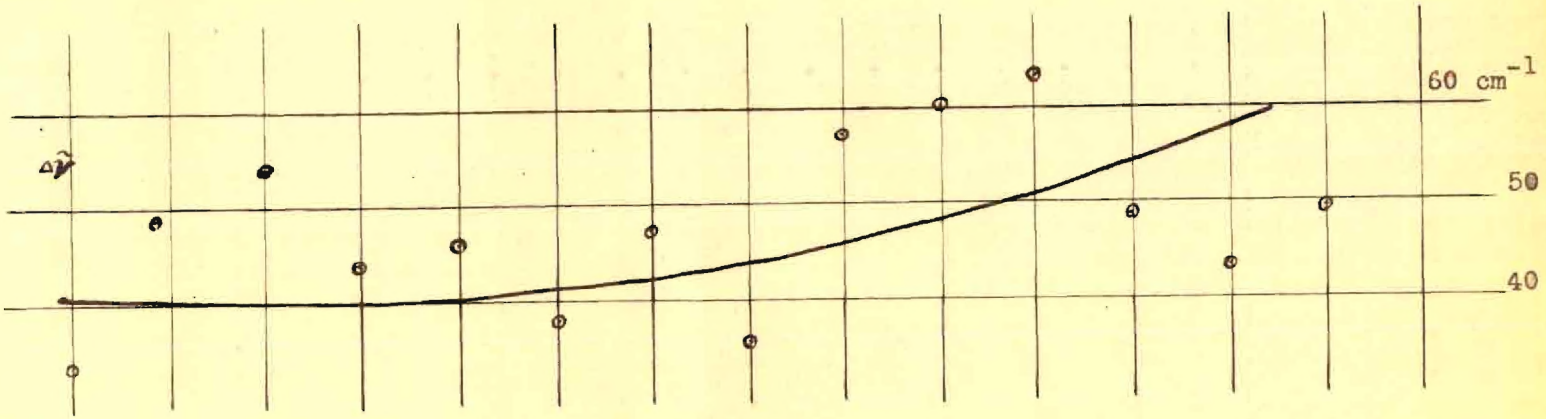

Figure 24b

DOUBLET SEPARATION OF NO_2 BANDS
BY HARTMANN FORMULA

curate determination of the wave lengths of the lines present in the ordinary spectrum. The channelled spectrum seems to partly resolve components that appear to be sub-bands but no evidence of resolution of rotational structure was found. Visual interpretation was limited to determining that several bands of about 10 cm^{-1} in width (121.5, in Figure 20) and a few of about 3 cm^{-1} (101.4, in Figure 20) appear to be resolved into at least two components. Thus an energy difference of about 1.5 cm^{-1} is measured which indicates a resolving power of about 0.2×10^5 at 4,000 Å. The Bausch and Lomb Large Littrow Spectrograph for the same slit, 0.08 mm, has a theoretical resolving power of about 0.1×10^5 at 4,000 Å. However, interpretation on any one photograph yields little information. Best results are obtained by comparing several photographs with different degree of contrast with the actual projection of the plate under different conditions of light intensity and enlargement. Little advantage seems to be gained by this technique for the preliminary analysis of absorption spectra. However, with sufficient experience in the techniques of interpretation, the channelled spectrum would probably yield more information on fine structure and more accurate values of molecular constants already known.

240699

BIBLIOGRAPHY

Burns, K., and Wm. F. Meggers, Publications of the Allegheny Observatory of the University of Pittsburg, 6, 105, (1925)

Fabry, Ch., Comptes Rendus des Seances de L'Academie des Sciences, 140, 1136, (1905)

Fabry, Ch., Les Applications des Interferences Lumineuses, (1927)

Fabry, Ch., and H. Buisson, Journal de Physics et le Radium, 9, 197, (1910)

Fizeau, Annales de Chimie et de Physique, 63, 393, (1861)

Harrison, Lord and Loofbourow, Practical Spectroscopy (New York: Prentice Hall, Incorporated, 1948) p. 561

Kayser, H., Tabelle der Schwingungszahlen, (Ann Arbor, Michigan: Edwards Brothers, Inc. 1944)

Meissner, Karl Willham, Journal of the Optical Society of America, 32 p. 191 (1942)

Tolansky, S., High Resolution Spectroscopy, (New York: Pitman Publishing Corporation, 1947) p. 104